Starting Control of Free Piston Stirling Linear Generator System Based on FOC

Qiaoling Yang, Kechun Zhang, Shenghui Guo, Boliang Song, and Xiaoyu Zhang

***Abstract*—Aiming at the problem of poor system dynamic performance caused by low parameter matching in the coordinated control of Stirling engine and linear generator in the starting stage control of free piston Stirling linear generator system, a joint control method of free piston Stirling permanent magnet synchronous linear generator system based on field orientation control is proposed, based on the theoretical derivation of the mathematical model of the system and the principle of controller parameters setting, the simulation experiments of the system starting stage under several Stirling engine working conditions are carried out under simulation. The experimental results show that the stability and rapidity of the system are improved, and the dynamic response speed of generator parameters under different working conditions is accelerated, what fully verifies the correctness and effectiveness of the method. It provides an effective way to improve the control performance of the system and stabilize the power generation operation.**

***Index Terms*—Parameter setting, Field orientation control, Double closed loop, Permanent magnet synchronous linear generator.**

I. INTRODUCTION

WITH the continuous attention of the state to the strategy of carbon neutralization and carbon peak, renewable energy power generation has ushered in space for further development. Among them, the free piston Stirling engine(FPSE), which belongs to the dish Stirling thermal power generation system, has great potential in space technology, nuclear energy application, solar energy application, heat recovery and other fields because of its simple structure, fuel diversification, cleanliness and efficiency [1]. Permanent magnet synchronous linear generator(PMLSG) has the advantages of fast response, high precision and low noise [2], which is widely used in military field, transportation system, CNC machine tool and other fields [3]. Combining the two can simplify the system structure, improve the system efficiency and stability, and effectively promote the development and utilization of new energy.

For the free piston Stirling power generation control system, the control strategy mainly includes starting stage control and generating stage control.[4] Quanrong Gong [5] adopted the three closed-loop structure of position, speed and current for the control system of free piston Stirling permanent magnet linear generator, mainly studied the smooth start of the system, and verified the correctness of the system only by the effect of position control in the start-up stage of the system and whether the speed end can decline smoothly. Shuqing Zhang [6] adopted the stroke current control strategy for the single-phase permanent magnet linear oscillation motor in the starting stage, and only the experimental results of stroke and frequency are used to reflect the dynamic response process of the system from the side. Yongheng Huang [7] used three closed-loop control of position, speed and current in the system starting stage to control the motor stroke and displacement by controlling the motor position and speed, so as to achieve the purpose of normal startup and operation of the system.

The above control strategy does not fully consider the dynamic response characteristics of generator electromagnetic thrust, $d-q$ axis current and other parameters in the system, so it is impossible to evaluate its dynamic performance from the perspective of the whole system. In this paper, a joint control method of free piston Stirling permanent magnet synchronous linear generator system based on field orientation control(FOC) is proposed, and the system controller parameters are adjusted to engineering practice, the simulation verification is carried out in the starting stage of the system, and the dynamic performance of the main parameters of the system in the process is comprehensively evaluated.

II. SYSTEM MATHEMATICAL MODEL

Linear motor evolved from rotating motor. When the rotating motor is cut along its radial direction and its circumference is expanded into a straight line [8], linear motor can be regarded as another existing form of rotating motor. The free piston Stirling power generation system mainly includes FPSE and PMLSG. PMLSG is a complex object with multivariable, strongly coupled, nonlinear and variable parameters[9]. It is assumed that the permanent magnet has no damping effect, the mover has no damping winding, and the magnetic field is sinusoidal distributed along the air gap, regardless of iron core saturation, eddy current and hysteresis

Manuscript received October 11, 2021; revised December 7, 2021; accepted February 11. date of publication June 25, 2022; date of current version June 18, 2022.

This work was supported in part by the National Natural Science Foundation of China under Grant 51767018, in part by the Scientific research project of Education Department of Gansu Province under Grant 2017A-012.

Qiaoling Yang, Kechun Zhang, Shenghui Guo, Boliang Song, Xiaoyu Zhang are with College of Electrical Engineering and Information Engineering, Lanzhou University of Technology, Lanzhou, 730050, China.(email: winds.qiaoer@163.com; ximenchuixueZKC@163.com; sbl6426295@163.com; bujidefengzxy@163.com; MMKKMKMK@126.com

(Corresponding Author: Qiaoling Yang)

Digital Object Identifier 10.30941/CESTEMS.2022.00026

loss.[10] The voltage equation and electromagnetic thrust equation of PMLSG in three-phase static coordinate system $a-b-c$ are as follows:

$$u_a = r_s i_a + \frac{d\psi_a}{dt} \tag{1}$$

$$u_b = r_s i_b + \frac{d\psi_b}{dt} \tag{2}$$

$$u_c = r_s i_c + \frac{d\psi_c}{dt} \tag{3}$$

$$F_e = \frac{1}{v}(E_a i_a + E_b i_b + E_c i_c) \tag{4}$$

Where u_a, u_b, u_c is the phase voltage of stator winding, i_a, i_b, i_c is the phase current of stator winding, ψ_a, ψ_b, ψ_c is ABC three-phase flux linkage, v is traveling wave magnetic field speed of linear motor [11], E_a, E_b, E_c is the back EMF of $a-b-c$ three-phase winding, F_e is electromagnetic thrust of linear motor, r_s is the resistance of stator.

In order to facilitate the order reduction and decoupling transformation of the mathematical model and the later design of the controller, it is necessary to transform the $a-b-c$ three-phase static coordinate system into $\alpha-\beta$ Under the two-phase stationary coordinate system, it is transformed from Park coordinate to $d-q$ synchronous rotating coordinate system. The Clark transformation process is as follows:

$$\begin{bmatrix} f_\alpha & f_\beta & f_0 \end{bmatrix} = T_{3S/2S}\begin{bmatrix} f_A & f_B & f_C \end{bmatrix} \tag{5}$$

Where $T_{3s/2s}$ is a coordinate transformation matrix, which can be expressed as:

$$T_{3S/2S} = \frac{2}{3}\begin{bmatrix} 1 & -\frac{1}{2} & -\frac{1}{2} \\ 0 & \frac{\sqrt{3}}{2} & -\frac{\sqrt{3}}{2} \\ \frac{\sqrt{2}}{2} & \frac{\sqrt{2}}{2} & \frac{\sqrt{2}}{2} \end{bmatrix} \tag{6}$$

The park transformation is as follows:

$$\begin{bmatrix} f_d & f_q \end{bmatrix}^T = T_{2S/2r}\begin{bmatrix} f_\alpha & f_\beta \end{bmatrix}^T \tag{7}$$

$$T_{2S/2r} = \begin{bmatrix} \cos\theta_e & \sin\theta_e \\ -\sin\theta_e & \cos\theta_e \end{bmatrix} \tag{8}$$

To sum up, the transformation from $a-b-c$ three-phase stationary coordinate system to $d-q$ two-phase rotating coordinate system can be expressed as:

$$\begin{bmatrix} f_d & f_q & f_0 \end{bmatrix}^T = T_{3s/2s}\cdot T_{2s/2r}\begin{bmatrix} f_A & f_B & f_C \end{bmatrix}^T \tag{9}$$

Where f represents motor voltage, current, flux linkage, and other variables.

By substituting PMLSG voltage equation, electromagnetic thrust and mechanical motion equation into the above formula, the mathematical model in $d-q$ coordinate system is :

$$L_d \frac{di_d}{dt} = u_d + \frac{\pi}{\tau} v\psi_q - r_s i_d \tag{10}$$

$$L_q \frac{di_q}{dt} = u_q - \frac{\pi}{\tau} v\psi_d - r_s i_q \tag{11}$$

$$F_e = \frac{3}{2}\frac{\pi}{\tau} P_n(\psi_f i_q + (L_d - L_q) i_d i_q) \tag{12}$$

$$M\frac{dv}{dt} = F_e - F_L - B_v v \tag{13}$$

Where P_n is the number of poles of the motor, τ is the pole pitch, M is the mover mass of the linear motor, F_L is the load resistance and B_v is the mechanical damping coefficient.

During the starting stage, the FPSE piston is driven to move by inverting the battery into AC, so as to achieve the purpose of stable operation of the engine. Therefore, for FPSE, it can be regarded as load relative to the system. The equation of FPSE power piston thrust F is as follows:

$$F = k(\frac{X_p}{2} - x) \tag{14}$$

Where k is the equivalent damping coefficient, X_p is the amplitude of piston and x is the piston displacement.

III. CONTROL SYSTEM DESIGN

Based on the idea that the armature current and excitation current of DC motor are perpendicular to each other, no coupling and can be controlled independently, FOC decouples the motor stator current into thrust component and excitation component in $d-q$ coordinate system through coordinate transformation, so that PMLSG has control performance similar to DC motor [12]. Based on the mathematical model in $d-q$ coordinate system, PMLSG can realize the decoupling of voltage, current, flux and other variables.[13] The control scheme with $i_d = 0$ is simple and has excellent characteristics.[14] Compared with PMLSG, it is the control with the largest thrust current ratio, and it is easier to realize motor speed regulation. To sum up, FOC can realize the decoupling of PMLSG control parameters and the control of thrust linearization in the system startup stage [15].

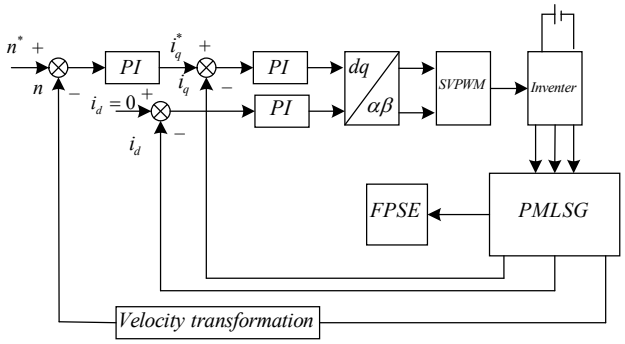

Fig. 1. i_d=0 control structure block diagram.

A. Design of current loop based on PI

The function of the current loop is to start with the maximum current during the motor starting stage, and quickly recover in case of external disturbance, accelerate the dynamic tracking response speed and improve the system stability.

Because the control method of $i_d = 0$ is adopted in this paper, the system characteristics of $d-q$ axis current loop are symmetrical and similar. Next, only the parameter setting method of q axis current PI control is analyzed. The parameters setting of d axis current PI control is similar to that of q axis current [16]. Due to the delay link and small inertia link of PWM control, the structural block diagram of q axis current loop is shown in the Fig. 2:

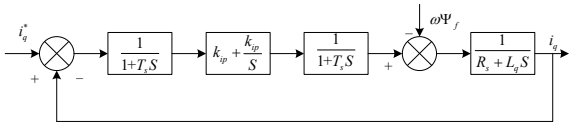

Fig. 2. structure diagram of q-axis current loop.

For simplified analysis, the disturbance caused by $\omega\psi_f$ is not considered .The simplified structure of q axis current loop can be obtained through a series of mathematical operations, as shown in the Fig. 3:

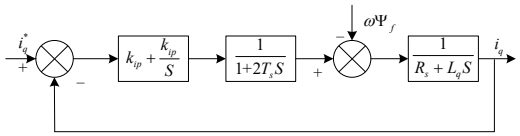

Fig. 3. simplified structure of q-axis current loop.

According to the above structural block diagram, the open-loop transfer function and closed-loop transfer function of the system are expressed as:

$$G_{(open)} = \frac{k_{ip}}{R_s\tau_i s(2T_s+1)} \tag{15}$$

$$G_{(\text{close})} = \frac{1}{1+\frac{R_s\tau_i}{k_{ip}}S+\frac{2T_sR_s\tau_i}{k_{ip}}S^2} \tag{16}$$

According to the dynamic performance index parameter table of typical type I system, the damping ratio $\varepsilon = 0.707$ is the best second-order system, thus:

$$\frac{2T_sk_{ip}}{R_s\tau_i} = \frac{1}{2} \tag{17}$$

The PI parameters of the current loop can be calculated as follows:

$$k_{ip} = \frac{L_q}{4T_s} \tag{18}$$

$$k_{ii} = \frac{k_{ip}}{L_q/R_s} \tag{19}$$

The output limiting of Simulink's own PI model only limits its output, and the internal integral term is not affected by it for continuous integration, which will lead to a large output of integral term, which cannot be desaturated when the ASR of the double closed-loop speed regulation system is desaturated. In order to obtain the same working characteristics of the actual controller and the designed PI controller, the current loop PI controller limit is set according to the limitation of the modulation mode, and the maximum SVPWM regulation is 1, that is, the limit amplitude is $U_{dc}/\sqrt{3}$.

B. Design of speed loop based on PI

For the PI controller used in the speed loop of the system, the system has no static error, the speed n can quickly follow the given speed n^*, reduce the speed error in the steady state, and has anti-interference effect when the simulated FPSE changes. The load resistance is introduced as a disturbance. Since the mechanical damping coefficient B_v is negligible in the project, the structural block diagram of the speed loop can be obtained, as shown in the Fig. 4:

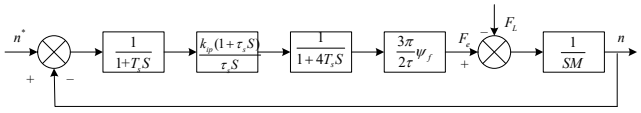

Fig. 4. structure diagram of speed loop

Ignoring the equivalent FPSE resistance, the current loop is equivalent to a small time constant $4T_s$ and small time constant of speed signal sampling T_s is combined to obtain a simplified speed loop structure block diagram, as shown in the Fig. 5:

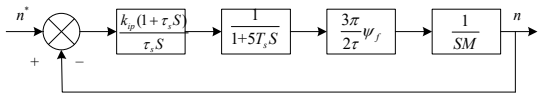

Fig. 5. simplified structure diagram of speed loop

According to the above structural block diagram, the open-loop transfer function is:

$$G_{(\text{open})} = \frac{\frac{3}{2}\pi\psi_f k_{sp}(\tau_s+1)}{M\tau\ \tau_s S^2(5T_sS+1)} \tag{20}$$

The intermediate frequency(IF) bandwidth of speed outer loop:

$$h = \frac{\tau_s}{T_{\varepsilon N}} \tag{21}$$

According to the open-loop function of typical Π system and its parameters setting relationship:

$$k_N = \frac{\frac{3}{2}\pi\Psi_f k_{sp}}{M\tau\ \tau_s} \tag{22}$$

The IF bandwidth $h = 5$ is generally taken in engineering application, and which is substituted into the above formula and derived as follows:

$$\frac{\frac{3}{2}\pi\Psi_f k_{sp}}{M\tau\ \tau_s} = \frac{h+1}{2h^2(5T_s)^2} \tag{23}$$

$$k_{sp} = \frac{2M\tau}{25\pi\Psi_f T_s} \tag{24}$$

$$k_{si} = \frac{k_{sp}}{\tau_s} \tag{25}$$

The above is the theoretical analysis and calculation of PI

controller parameters of current loop and speed loop, and the actual operation of the system is often different from the theoretical analysis, so the parameters should be adjusted appropriately according to the actual situation in practical application.

C. SVPWM algorithm

SVPWM is based on the principle of average equivalence. By combining the basic voltage vectors within, the average value is equal to the given voltage vector in a switching cycle T_S. Advantages:1)PWM has better harmonic elimination effect than SPWM, improves voltage utilization and is easy to realize; 2)PWM algorithm improves dynamic response speed of motor and reduces motor torque ripple; 3VPWM is suitable for digital control system. The synthetic voltage space vector diagram under the complex plane is shown in the figure:

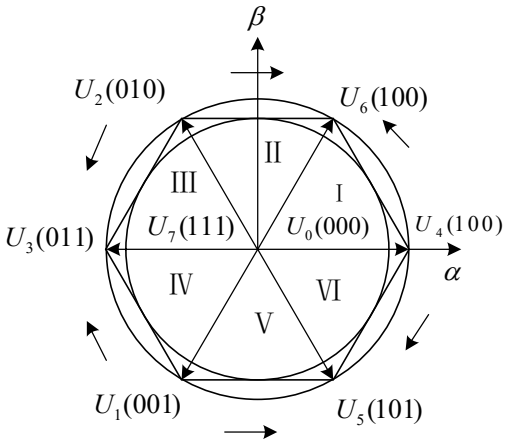

Fig. 6. Space vector diagram of synthetic voltage.

IV. SIMULATION ANALYSIS

The simulation block diagram of the starting stage control of free piston Stirling power generation system based on FOC is shown in the figure. Motor simulation parameters: P_n=2, $M=0.824kg$, $L_d=L_q=1.77mH$, $\tau=9mm$, $r_s=0.448\Omega$ $\psi_f=0.0513Wb$, $B_v=10$. Because the complexity of FPSE mathematical model and the limitation of experimental conditions, the equivalent working conditions of FPSE under three idealized conditions of $F=100N$; $F=100\sin(2*pi*30*t)N,(0\le t\le 0.2s)$; and $F=800t(0\le F\le 100N),(0\le t\le 0.2s)$ are simulated and analyzed respectively.

Figure 8-10 shows the motor current waveform under different thrust of the ideal FPSE. In Figure 8, the system reaches stable operation state at 0.004s. Figure 9 since the equivalent FPSE is a sinusoidal thrust, the system also changes sinusoidally on the basis of stable operation state. In Figure 10, the motor current increases in proportion to the thrust of FPSE, and the system operates stably at 0.125s.

The speed loop belongs to the second-order system. From the amplitude frequency curve and phase frequency curve of the second-order system, the main parameters affecting the second-order system are frequency and damping ratio. When the damping ratio is 0.6~0.8, that is, the system is in the

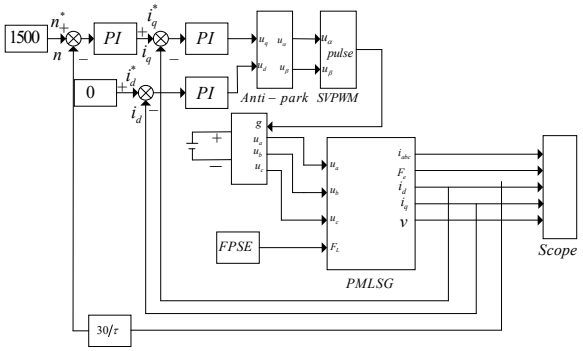

Fig. 7. Simulation system diagram.

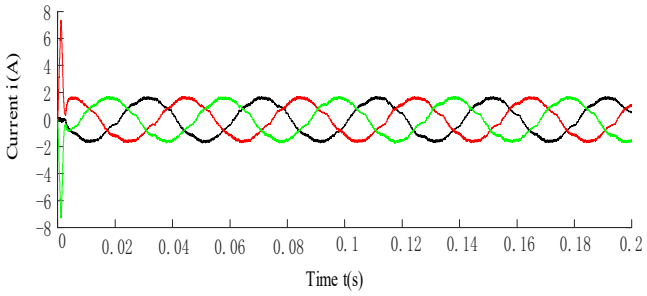

Fig. 8. Current diagram of $F=100N$ motor.

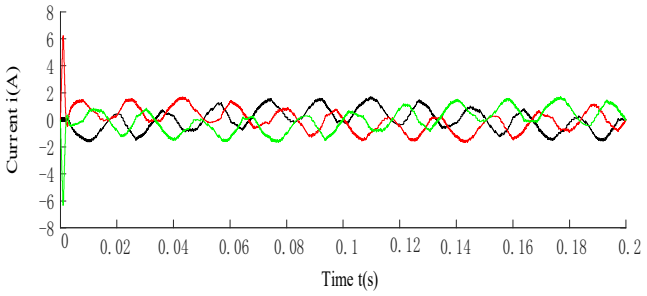

Fig. 9. Current diagram of $F=100\sin(2*30*t)N,(0\le t\le 0.2s)$ .motor.

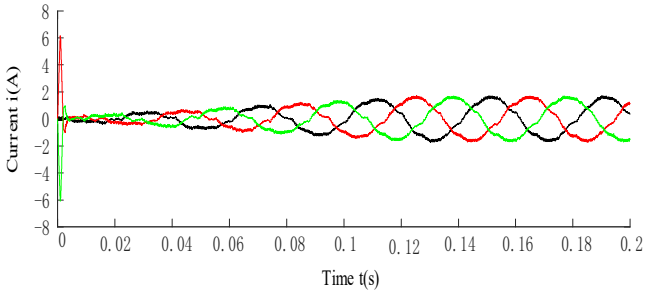

Fig. 10. Current diagram of $F=800t(0\le F\le 100N),(0\le t\le 0.2s)$ motor.

underdamped state, better comprehensive performance can be obtained. In engineering application, damping ratio ε is general 0.707. It can be seen from the speed waveform converted from the speed of linear motor to rotating motor in Figure 10 that when $F=100N$, the overshoot:

$$\sigma\%=\frac{h(t_p)-h(\infty)}{h(\infty)}\times 100\%=16\% \tag{26}$$

Since the allowable value of speed overshoot in the motor control system is generally 20%~30%[17], the above shows that the system has good stability. When $F=100\sin(2*30*t)N,(0\le t\le 0.2s)$, due to the sinusoidal

change of F, the motor speed also changes sinusoidally. When $F=800t(0\le F\le 100N),(0\le t\le 0.2s)$, the speed overshoot increases slightly.

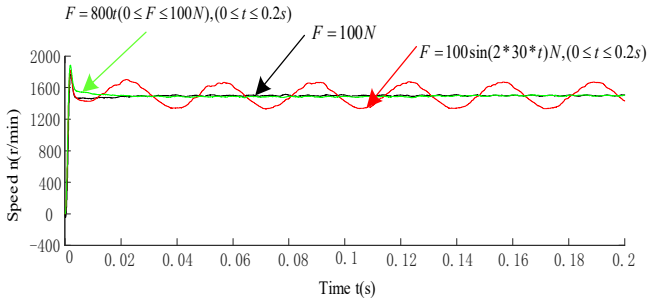

Fig. 11. Motor speed diagram.

As can be seen from Figure 12, when the control system adopts FOC, in terms of electromagnetic thrust, when $F=100N$, the system reaches a stable operation state at 0.004s, with fast instantaneous start and small perturbation. It is suitable for control occasions requiring rapid response to electromagnetic thrust. It can be seen from (13) that the system operates stably and ignores B_v, $F_e\approx F_L=100N$. When $F=100\sin(2*30*t)N,(0\le t\le 0.2s)$ reaches the peak value and $F=800t(0\le F\le 100N),(0\le t\le 0.2s)$ reaches the target value of 100N, the simulation results are consistent with the theoretical calculation.

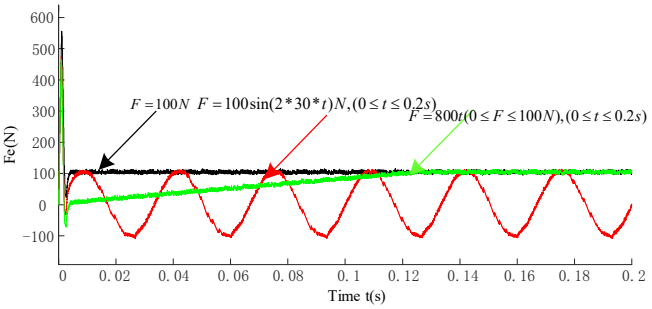

Fig. 12. Electromagnetic thrust diagram of motor

From Figure 13, the current waveform of motor i_q can verify the correctness of $i_d=0$ control method and motor model. When $F=100N$, refer to (12), which is the electromagnetic thrust equation of linear motor, $i_q=2\tau F_e/3\pi\psi_f$ is calculated as 2.0 A, which is consistent with the simulation results. And it can be seen from the above formula that in the permanent magnet motor ψ_f is constant, the change of i_q with the change of the electromagnetic thrust F_e. The above analysis can also be verified from $F=100\sin(2*pi*30*t)N,(0\le t\le 0.2s)$, $F=800t(0\le F\le 100N),(0\le t\le 0.2s)$.

Figure 14-15 compares the PMLSG speed and electromagnetic thrust waveforms based on FOC system and open-loop control system respectively. It can be clearly seen from the figure that the free piston Stirling power generation system designed in this paper has good stability and rapidity under three working conditions of $F=100N$ $F=100\sin(2*pi*30*t)N,(0\le t\le 0.2s)$ and $F=800t(0\le F\le 100N),(0\le t\le 0.2s)$.

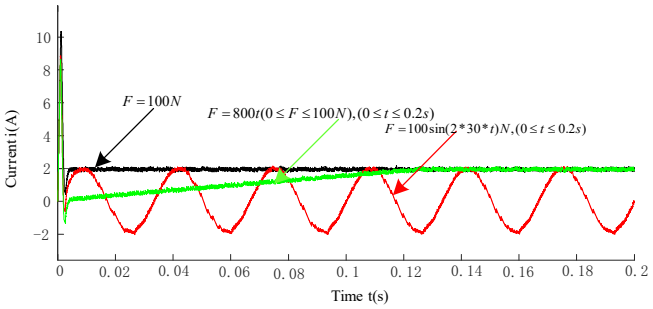

Fig. 13. Motor i_q graph.

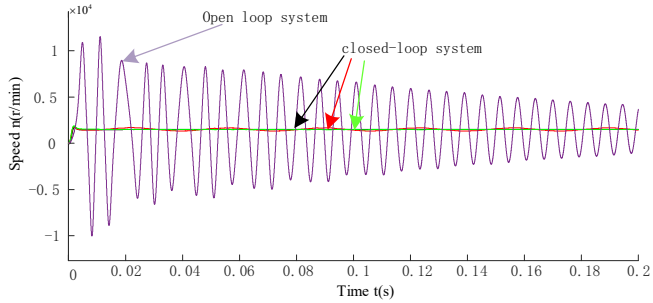

Fig. 14. Motor speed diagram of different systems.

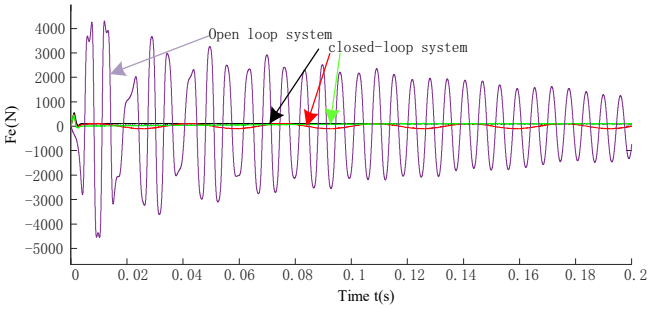

Fig. 15. Electromagnetic thrust diagram of motors in different systems.

V. CONCLUSION

Through the simulation of starting control of power generation system under three equivalent working conditions of engine power piston thrust $F=100N$; $F=100\sin(2*pi*30*t)N,(0\le t\le 0.2s)$ and $F=800t(0\le F\le 100N),(0\le t\le 0.2s)$, it is shown that the joint control method of free piston Stirling permanent magnet synchronous linear generator system with $i_d=0$ FOC can effectively improve the stability and rapidity of the system in the starting stage. In the dynamic response process of PMLSG parameters under different working conditions of FPSE, the parameter setting method of system controller derived from theory can effectively guide the experimental parameter setting, and has good engineering application value.

REFERENCE

[1] B. J. G. de la Bat, R. T. Dodson, T. M. Harms, A. J. Bell, “Simulation, manufacture and experimental validation of a novel single-acting

free-piston Stirling engine electric generator", *Applied Energy,* vol. 263, Jan. 2020.

[2] J. Jiang, F. Lin, B. Li, J. Xiao, H. Zhang and P. Ye, "A Two-step Tuning Method of Control Parameters for Permanent Magnet Synchronous Linear Motor", *2021 IEEE 5th Advanced Information Technology, Electronic and Automation Control Conference (IAEAC)*, vol. 5, pp. 1029-1034, Mar. 2021.

[3] F. Xiang, M. Z. Xu. "Direct thrust control of permanent magnet linear synchronous motor based on improved sliding mode speed controller", *Motor and Control Applications*, vol. 46, pp. 38-43, 2019.

[4] J. G. Zheng. "Basic research on free piston Stirling power generation system", M.S. thesis, Dept. Electron. Eng., HIT Univ., Harbin, China, 2017.

[5] Q. R. Gong. "Research on control system of free piston Stirling permanent magnet linear generator，" M.S. thesis, Dept. Electron. Eng., HIT Univ., Harbin, China, 2010.

[6] S. Q. Zhang. "Research on control system of free piston Stirling permanent magnet linear generator," M.S. thesis, Dept. Electron. Eng., HIY Univ., Harbin, China, 2014.

[7] Y. H. Huang. "Research on control system of permanent magnet linear generator", M.S. thesis, Dept. Electron. Eng., HIT Univ., Harbin, China, 2011.

[8] C. Y. Du. "Research on control strategy of permanent magnet synchronous linear motor", M.S. thesis, Dept. Electron. Eng., NCUT Univ., Beijing, China, 2021.

[9] Z. Li, Q. S. Zhang, J. F. An, et al. "Terminal sliding mode speed control method of permanent magnet synchronous linear motor based on adaptive parameter identification", *Mechanical Engineering*, vol. 13, no. 4, pp. 1-11, Mar. 2021.

[10] G. J. Su, H. M. Li, Z. Li, et al. "Research on Model-Free Current Control of Permanent Magnet Synchronous Linear Motor", *Transactions of China Electrotechnical Society*, vol. 36, no. 15, pp. 3182-3190, Aug. 2021.

[11] J. Zhao, L. Wang, L. Xu, et al. "Uniform Demagnetization Diagnosis for Permanent-Magnet Synchronous Linear Motor Using a Sliding-Mode Velocity Controller and an ALN-MRAS Flux Observer", *IEEE Transactions on Industrial Electronics*, vol. 69, no. 1, pp. 890-899, Jan. 2022.

[12] L. Yuan, B. X. Hu, K. Y. Wei. "Control principle and MATLAB simulation of modern permanent magnet synchronous motor", Beijing: Beijing University of Aeronautics and Astronautics Press, 2016, pp. 66-79.

[13] Z. Y. Sun. "Vector control of permanent magnet synchronous linear motor", M.S.thesis, Dept. Electron. Eng.，LUT Univ., Lanzhou, China, 2009.

[14] X. Chen, Y. D. Zhao. "Simulation analysis of electromagnetic and control strategy of permanent magnet synchronous motor", *Machine Tool & Hydraulics,* vol. 49, no. 3, pp. 159-165, Feb. 2021.

[15] X. F. Zhai, J. H. Zhang, J. H. Zhao. "The Matlab Simulation of the Permanent Magnetic Linear Synchronous Motor of Positioning Experiment", *Marine Electric & Electronic Technology,* no. 4, pp. 6-9, Apr. 2006.

[16] J. H. Qiao, L. Q. Wang. "Simulation of Double Closed Loop Control System for Permanent Magnet Synchronous Motor", *Henan science and technology*, vol. 2, no. 5, pp. 44-47, Feb. 2021.

[17] H. Shen, W. Zhang, W. R. Tan, S. H. Dang, "Analysis of Thrust and Speed Variation of Permanent Magnet Synchronous Linear Motor under Variable Load", *Journal of Lanzhou University of Technology,* vol. 47, no. 2, pp. 54-59, Apr. 2021.

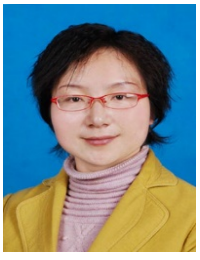

QiaoLing Yang received her doctorate in 2020 in renewable energy power generation and smart grid from Lanzhou University of Technology. Now she is a teacher of Lanzhou University of Technology, and engaged in the fields of control and power electronics and power transmission in teaching and scientific research work 20 years.

Kechun Zhang was born in Gansu,China, in1998. He received his bachelor's degree from Lanzhou University of Technology in 2020 and began studying for a master's degree in the same year. His main research direction is the control of permanent magnet linear motor.

Shenghui Guo was born in Qinghai, China, in 1997. He received his bachelor's degree from Yuncheng University in 2019 and is now pursuing his master's degree at Lanzhou University of Science and Technology. His main research direction is the design of permanent magnet vernier motor.

Boliang Song was born in Heilongjiang Province, China, 1995. He joined the school of Electrical Engineering, Lanzhou University of Technology. His main field of interest is design and control of linear motor.

Xiaoyu Zhang was born in Henan Province, China, in 1997. He is presently pursuing a master's degree in electrical engineering, Lanzhou University of technology. His current research interests include microgrid and smart grid, and optimal dispatching of new energy.